LAWRENCE
LIVERMORE
NATIONAL
LABORATORY

LLNL-JRNL-840344

Soil management legacy interacts with wheat genotype to determine access to organic N in a dryland system

C. Kelly, P. F. Byrne, M. E. Schipanski, J. Schneekloth, F. Calderon, S. J. Fonte

September 27, 2022

Agriculture, Ecosystems and Environment

Disclaimer

Title: Soil management legacy interacts with wheat genotype to determine access to organic N in a dryland system

Authors: Courtland Kelly[1,2], Patrick F. Byrne[2], Meagan Schipanski[2], Joel Schneekloth[3], Francisco Calderón[4], Steven. J. Fonte[1]

[1] Physical and Life Sciences Directorate, Lawrence Livermore National Laboratory, Livermore, CA

[2] Department of Soil and Crop Sciences, Colorado State University, Fort Collins, CO

[3] US Central Plains Research Station, Colorado State University, Akron, CO

[4] Columbia Basin Agricultural Research Center, Oregon State University, Adams, OR, USA

LLNL IM Release #: LLNL-JRNL-840344

Abstract:

Organic nutrient management through the application of compost and/or cover crops provides mineralizable sources of nutrients for plants while often building soil organic matter (SOM) and various aspects of soil health. Variability in nutrient acquisition strategies between crop genotypes may confer advantages under different soil health contexts and could be important for crop selection and breeding, but crop response under field conditions remains unexplored. We investigated the ability of different genotypes of winter wheat (*Triticum aestivum* L.) to access nitrogen (N) from newly added cover crop residues in two soils with contrasting levels of SOM and biological activity. We planted three previously characterized wheat genotypes in a long-term dryland compost amendment field trial: 1) Byrd (current, deep roots, low exudation), 2) Cheyenne (historic, drought susceptible, intermediate exudation), and 3) Snowmass (current, drought-susceptible, high exudation). ^{15}N-labelled cover crop residue was added to each plot and traced into wheat tissue. In the low SOM soil, the high exudate genotype Snowmass and historic genotype Cheyenne took up the most residue-derived N (6.4-8.1 kg N ha^{-1}) compared to the low-exudate genotype Byrd (4.4 kg N ha^{-1}), suggesting a strong exudate effect in the more carbon-limited soil. However, the low-exudate, deep rooted genotype, Byrd, took up the most residue N in the high SOM soils (4.6 kg N ha^{-1} vs. 2.8 and 3.3 hg N ha^{-1} for Cheyenne and Snowmass, respectively), which indicated higher native N cycling activities and great importance of drought resistance. Enzyme activity, inorganic N, and microbial communities were not influenced by genotype, though did show strong effects of compost application legacy. Our results show that belowground allocation strategies that favor microbial stimulation may be less successful under water limitation, especially when high SOM can support mineralization of residue N without added investment in root inputs. Increased soil health through SOM-building management likely enhances nutrient cycling, and may better support root strategies that invest less in microbial stimulation in favor of other limiting resources.

Keywords: *Triticum aestivum*; soil organic matter; compost; cover crop; nitrogen mineralization; organic nutrient management

1. Introduction:

Improved soil health is a critical management goal for farmers, policy-makers and society, as agriculture is increasingly asked to provide environmental services as well as sustain food production. While there is on-going and vigorous debate regarding the definition and measurement of soil health (Janzen et al., 2021), certain practices, such as the addition of organic amendments, is generally thought to contribute to soil health by increasing levels of soil organic matter (SOM) and biological activity, while reducing losses of reactive nitrogen (N) (Xia et al., 2017). Organic amendments such as compost, manure, and leguminous cover crops (green manure) are commonly utilized in organic agriculture to support crop nutrition where synthetic fertilizers are not permitted. Composted manure primarily contains organic, mineralizable N, which can provide a slow release of N during the growing season. Cover crops may also supply sufficient N to meet crop demands if cover crop biomass production and N fixation is adequate (Tonitto et al., 2006). Along with supplying crop nutrients, organic amendments can rapidly improve many soil properties related to soil structure, water dynamics, and nutrient cycling (Six et al., 2004).

In addition to nutrient inputs, plant roots can also affect SOM dynamics and microbial communities through exudation. Roots of different plant types can stimulate soil N mineralization, but the direct link to plant N availability and uptake remains unclear (Gan et al., 2022; Huo et al., 2017). Root effects on N mineralization are mediated through stimulation and/or selection of the rhizosphere microbial community and N cycling activities (Qu et al., 2020; Yu et al., 2021). There is increasing evidence that plant rhizosphere microbiomes show species and even genotypic specificity in selecting microbial taxa, which can perform soil functions that contribute to plant success (Sánchez-Cañizares et al., 2017). For example, plants have been shown to use root exudation to recruit microbial taxa that assist in nutrient mobilization, such as phosphorous (P) solubilization or N mineralization, or to exclude pathogenic organisms (Fitzpatrick et al., 2018; Mendes et al., 2018).

Rhizosphere microbial interactions may be an integral part of plant resource acquisition strategies that are just now being integrated into existing resource allocation frameworks. For example, the root economic spectrum focuses on the amount and structure of root tissues allocation in response to resource gradients (Reich, 2014). However, recent work on root traits has unearthed evidence of another “collaboration” axis, where species with high microbial associations have smaller root systems but produce more exudates (i.e., collaborative) to increase

nutrient availability closer to the root (Bergmann et al., 2020; Wen et al., 2022). Indeed, evidence from >1800 plant species supports a collaboration gradient with regard to root-microbial symbioses (Bergmann et al., 2020).

Root exudation is a complex process controlled by many different genetic pathways, and is likely subject to many of the same selection pressures as other plant traits (Schmidt et al., 2016). It has been postulated that more recent efforts in plant breeding, especially under soil environments with high inputs of inorganic nutrients, may have disrupted co-evolutionary processes between plant roots and rhizosphere microbial communities, with potential to decrease crop access to organic nutrient inputs (Pérez-Jaramillo et al., 2016; Schmidt et al., 2016). Work in several crops, including maize and winter wheat, have found a shift in root-associated microbial communities in modern vs. older genotypes (Hetrick et al., 1993; Schmidt et al., 2020; Tkacz et al., 2020). This work suggests that recent breeding efforts may be responsible for unintentional selection away from historical root-microbial interactions, which could affect crop fitness in soils with high inputs of organic nutrient sources.

As agroecosystems move to improve environmental health through greater reliance on cycling of organic nutrients, certain crop genotypes and traits may be better suited to participating in and benefitting from microbially-mediated nutrient cycling activities. Genotype-level variation in root architecture and exudate dynamics have been found in winter wheat (*Triticum aestivum* L.), an important global staple crop (Kelly et al., 2022b). These differences in root traits can confer varying levels of drought resistance and N use efficiency (Becker et al., 2016; Foulkes et al., 2009) and likely affect the rhizosphere microbiome, with important implications for nutrient cycling and plant access to organic nutrient sources. Different cultivars of durum wheat (*Triticum durum* L.) have demonstrated unique exudation profiles related to root morphology and rhizosphere community composition (Iannucci et al., 2021), but the implications for rhizosphere functions like nutrient cycling remain poorly understood. It is especially critical to investigate root-rhizosphere dynamics in the field to understand these relationships in realistic scenarios, but there is very little research linking root traits to rhizosphere functions in a field setting.

The objective of this study was to assess the relative ability of distinct winter wheat genotypes to access residue-derived N under different soil health contexts. We hypothesized that wheat genotypes with higher levels of exudation and less intensive breeding (i.e., older) will

perform better in a high-SOM context since greater investment in microbial interactions should provide greater access to organic nutrients. More specifically, we hypothesized that genotypes with higher exudation rates will stimulate greater hydrolytic enzyme activity and available N, driven by distinct microbial communities. To test these hypotheses, we utilized a long-term compost amendment field trial to assess the effects of different levels of soil health, mainly determined by differences in SOM and biological activity. Within this experiment, we planted three different genotypes of winter wheat, selected from previous research demonstrating differing belowground C allocation patterns. We applied ^{15}N-labelled cover crop residue to the soil to trace the mineralization and uptake of residue-N into wheat tissue, and related these dynamics to microbial community structure, enzyme activity, and available inorganic N in the soil. Together, these methods allow us to relate crop genotype differences in belowground allocation to microbial community structure and function, in the context of N flows and transformations in an agroecosystem.

Methods

2.1 Site and experimental design

The study site was a long-term (10 yr) semi-arid dryland experiment established in 2010 at the USDA-ARS Central Great Plains Research Station in Washington County, Colorado (40°09'22.4"N 103°08'26.1"W, altitude 1, 384 m). Two soil types are present at this location: Weld silt loam (fine, smectitic, mesic Aridic Argiustoll) and a Rago silt loam (fine, smectitic, mesic Pachic Argiustoll). Average high and low temperatures range from 32°C in July to -10°C in January, with average annual rainfall of 417.5 mm (Table S2). During the two study years considered here, total annual precipitation was 273 in 2020 and 461 mm in 2021 (Table S2). This study employed a two-year crop rotation with alternating years of winter wheat and bare fallow. The fields were managed without synthetic fertilizers or herbicides, utilizing shallow sweep tillage (8 cm depth) twice each summer for weed control (Calderón et al., 2018). The only exception was in 2020, where glyphosate was applied twice before wheat planting in September to control aggressive weed populations and avoid tillage (and associated soil moisture loss). The plots utilized in this study included contrasting soil health management practices, with biennial applications of beef feedlot compost applied before wheat planting at a rate of 109 Mg

138 ha^{-1} (5x), which corresponds to roughly five times the expected crop N demand, versus a control
139 with 0 Mg ha^{-1} (0x). Both phases of the crop rotation are present every year, with all compost
140 treatments and phases present in each of four replicate blocks. The compost, 80% dry matter
141 with a total N content to 1.9% and a C:N ratio of 9.0, was applied in 2019 before wheat planting.
142 Additional details on agronomic management, soil properties and compost composition are
143 reported by Calderón et al. (2018) and Liu et al., (2021), as well as in Table S1.
144 Within the 0x and 5x compost plots, three sub-plots (5.5 x 1.6 m) were established within
145 the winter wheat phase of the rotation in 2019 and again in 2020. The three sub plots in each
146 main plot were randomly assigned one of three winter wheat cultivars selected for this study
147 based on diverging root traits reported by Kelly et al. (2022b). This study design was repeated
148 over two growing seasons: 2019-2020, and 2020-2021. In each year, the wheat was planted in
149 plots following a 14-month bare fallow to simulate the wheat-fallow rotation system common in
150 the region. Therefore, the planted plots differed between the years, though they were adjacent
151 within the same block layout. Wheat planting occurred on Sept 25, 2019 and Sept 24, 2020
152 using a cone planter (Hege Equipment Ltd., KS, USA) with 19 cm row spacing, 4 cm planting
153 depth, and planting density of 33 seeds m^{-1} of row (175 seeds m^{-2}).
154 The three cultivars planted in the current study were: 'Byrd', a current hard red semi-
155 dwarf winter wheat (Haley et al., 2012); 'Snowmass', a current hard white semi-dwarf winter
156 wheat (Haley et al., 2011); and 'Cheyenne', a tall historic variety released in 1930 (Table 1).
157 Byrd is considered a drought-tolerant genotype and has been previously shown to have relatively
158 long, thin roots with low levels of exudation; Snowmass is drought-susceptible with short, coarse
159 roots and high exudation; Cheyenne has intermediate root length and exudation (Becker et al.,
160 2016; Kelly et al., 2022b, 2022a).
161 In 2019 prior to compost application, a 3 m^2 microplot was established in the center of
162 each cultivar sub-plot where compost was excluded to avoid an additional new N source. One
163 day prior to wheat planting in both 2019 and 2020, soil from a 1m^2 microplot was mixed with
164 ^{15}N-labelled cover crop material to a depth of 15 cm. The cover crop residue was a mixture of
165 hairy vetch (*Vicia villosa* L.) and Triticale (x *Triticosecale* Wittmack) and was applied at a rate
166 of 1600 kg ha^{-1} (dry biomass), which is within the range of typical cover crop biomass
167 production in the region (Kelly et al., 2021). The cover crop mixture was grown in pure sand
168 supplied with N-free Hoagland's solution (Hoagland & Arnon, 1950) amended with 9 atm%^{15}N-

KNO_3 (Cambridge Isotope Laboratories, MA, USA). Cover crop material was prepared by oven drying at 50 °C and coarsely chopping to ~ 5 cm pieces; in 2020, the root material was coarsely ground to better facilitate even distribution in the microplot. Final enrichment for the cover crop material was 8.03 atm% ^{15}N, while total N concentration of the material was 23 g kg^{-1}, for an N application rate of 36.8 kg ha^{-1}.

Due to extremely dry conditions during both years of the study, supplemental irrigation was applied to the treatment plots using drip tape spaced at 30 cm intervals running the length of the plots, as well as 1.5 m of buffer on either side. In early November 2019, 2 cm of water was applied through surface drip irrigation to aid in stand establishment. In 2020, a larger quantity of water was added to alleviate extreme drought conditions; 7.6 cm of water was applied using the same drip tape method in late August, and an additional 2.5 cm of water was applied by hand in to the microplots in late October to replace evaporative losses from mixing in the cover crop residues during plot preparation.

2.2 Soil and plant sampling

We collected rhizosphere soil samples twice during the growing season, once at tillering (early May) and again at heading/flowering (early June) in both sampling years. The root systems of three separate plants from each cultivar sub-plot (outside the microplots) were gently excavated down to about 15 cm, shaking off loose soil, and placing the root system with adhered soil in a sterile Whirlpack bag. The loosely-adhered soil that fell off the root system was also collected as "root zone" soil in a zip-top bag for nutrient analysis. All samples were kept on ice for transport back to the lab. In the lab, we dislodged rhizosphere soil from roots by squeezing the root bag to break up aggregates. We transferred ~0.3 g of rhizosphere soil into Zymo BeadBashing tubes, added 700 mL BeadBashing Buffer, vortexed briefly, and kept frozen at -20 °C for DNA extraction (see below). We also transferred a 1 g subsample of rhizosphere soil into 120 mL specimen cups and kept at 4 °C for enzyme analysis (see below). "Root zone" soil was 2-mm sieved and ~8 g of fresh soil extracted with 40 mL 2 M KCl for inorganic N analysis. Extracts were kept frozen until analysis for nitrate and ammonia on an Alpkem Flow Solution IV system (O.I. Analytical, College Station, TX). Soil moisture content was also determined on this soil using a ~50 g subsample.

The final sampling occurred at wheat harvest (mid-July). Two 1-m rows of wheat were harvested from the main plot by cutting the wheat plants ~5 cm from the soil surface for determination of plant biomass and grain yield. Wheat biomass and grain samples were oven-dried at 55 °C, weighed, grain was cleaned using a belt thresher (Agriculex, Ontario, CA) and the grain weighed separately from the straw. From within the cover crop microplots, we harvested wheat plants from the center three rows of the plots, at least 15 cm away from the plot edge to minimize edge effects. These samples were also oven-dried at 55 °C and threshed to separate wheat grain from straw.

Wheat straw and grain samples from within the microplots were ground and analyzed for total C, total N, and ^{15}N signature at the UC Davis Stable Isotope Facility using a PDZ Europa 20-20 isotope ratio mass spectrometer (Sercon, Ltd., Cheshire, UK), which allowed us to determine the amount of added cover crop-derived N taken up by the wheat plants.

Immediately following wheat harvest, in-row soil cores (3.8-cm diameter) were taken down to 30 cm with a tractor-mounted hydraulic probe (Giddings, Windsor, CO, USA). Two cores were taken from within each microplot and kept on ice for transport back to the lab. In the lab, bags containing cores were weighed for determination of bulk density, and then soil was passed through a 2-mm sieve and wheat roots removed. A subsample of fresh soil was dried at 105 °C for soil moisture.

2.3 Microbial communities and activity

Enzyme activity and amplicon sequencing were conducted on rhizosphere soil collected at the tillering and flowering timepoints. Hydrolytic enzyme activity was measured fluorometrically following German et al. (2011) to assess the enzyme activities: *L*-leucine aminopeptidase (LAP), *L*-Tyrosine aminopeptidase (TAP), and N-Acetyl-β-D-glycosaminidase (NAG); β-1,4-glucosidase (BG) and β-D-cellobiosidase (CB); phosphatase (PHOS). LAP, TAP and NAG assess N cycling and mineralization potentials; BG and CB assess labile and more structural C cycling, respectively; and PHOS targets phosphorous (P) cycling. Briefly, 1 g fresh soil was blended with 120 mL 50 mM sodium acetate buffer for 1 min. to create soil slurries. We combined 200 μL soil slurry with 50 μL 200 μM fluorescent substrate solution in replicates of 16, and incubated for 4 hours at 25 °C. Control reactions were included in each plate: un-bound 4-methylumbelliferone or methylcoumarin fluorescing agent with the soil slurry to estimate

quenching, and substrate combined with soil-free buffer to estimate background fluorescence. Fluorescence was measured on a microplate fluorometer (Infinite M200, Tecan, Switzerland) with 365 nm excitation and 450 nm emission filters.

We extracted genomic DNA from rhizosphere soils using the Quick-DNA Fecal/Soil Microbe kit (Zymo Research Corporation, Irvine, CA) following manufacturer's instructions. Amplicon libraries were prepared for the 16S rRNA region using the 515/806 Earth Microbiome Project standard primer pair (Caporaso et al., 2011), and the V3-V4 region of the ITS gene (ITS-2; White et al., 1990). Extracted DNA was quantified using the Qubit ds DNA High Sensitivity quantification system (Invitrogen). Sequencing was conducted at the University of Colorado – Anschutz using an Illumina MiSeq (2 x 250 bp). Sequence data will be uploaded to the NCBI SRA database under project ID PRJNA735275 upon acceptance for publication.

2.4 Isotope calculations

By quantifying the amount of ^{15}N in wheat grain and straw samples, we were able to determine the relative contribution of our added cover crop residue to the N in these tissues. The relative proportion of N derived from the ^{15}N-labelled cover crop residue in the wheat plants was calculated using the mixing model:

$$f_{label} = \frac{(atm\%_{sample} - atm\%_{control})}{(atm\%_{label} - atm\%_{control})}$$

where f_{label} is the relative contribution of the labeled cover crop to the sample, $atm\%_{sample}$ is the atom% of the sampled material, $atm\%_{control}$ is the atom% of the natural abundance soil, and $atm\%_{label}$ is the atom% of the ^{15}N labelled cover crop residue. Due to slight differences in the background ^{15}N values of the different soil treatments (0x vs 5x; Table S1), a different natural abundance end member was used for samples from each of these soils. We calculated the total uptake of cover crop-derived N in wheat by multiplying the f_{label} value above and multiplying it by the concentration of N in the sample (wheat grain or straw).

2.5 Statistical analysis of plant and soil metrics

We used two-way ANOVA to test the effect of wheat genotype and soil treatment (compost vs. no compost) on various metrics of wheat performance and N utilization. For soil enzyme activity and inorganic N measurements, the sample period (tillering or

heading/flowering) was also included as a fixed effect. Block was included as a random effect for single-timepoint measures, while plot was included in the models for enzyme activity and inorganic N measures that were repeated throughout the growing season. The model was implemented using the *lmer* function in the *lme4* package, and the *lmerTest* package used for ANOVA implementation (Bates et al., 2015; Kuznetsova et al., 2017). An alpha value of $p < 0.1$ was used to evaluate statistical significance to account for inherent variability in field conditions. Log transformations were applied as needed to meet the assumptions of ANOVA. All statistical analyses were performed in R version 4.0.3 (R Core Team, 2020), and plots were constructed using *ggplot2* (Wickham et al., 2018).

2.6 Microbial community analysis

Amplicon sequences data (16S and ITS) were processed using QIIME2 2 v 2019.2. Denoising was performed using DADA2 on paired-end reads for 16S data and forward reads for ITS data to improve feature clustering (Callahan et al., 2016). 16s forward and reverse reads were trimmed to 247 and 186 base-pairs, respectively, and ITS forward reads trimmed to 200 base-pairs. We used a Native Bayes taxonomic classifier trained on our study primer pairs through QIIME2 (Bokulich et al., 2018) that utilized the SILVA and UNITE reference databases for bacteria/archaea sequences and ITS sequences, respectively (Abarenkov et al., 2020; Quast et al., 2013). Features that only appeared once and without classification past Kingdom were removed from both datasets, with chloroplast and mitochondrial sequences removed from the 16S dataset. Sequence data is available in the NCBI SRA under PRJNA735275 SUB11809024.

We computed alpha diversity metrics on rarefied data to account for uneven sampling depth using the QIIME2 Core Metrics function (Bolyen et al., 2019). We completed additional multivariate analysis on family-level data after completing additional filtering steps: features that appeared less than 4 times in 20% of samples were excluded, as well as 10% lowest variance features according to inter-quartile range, as these are unlikely to show treatment effects. The abundance data was then scaled using the Cumulative Sum of Squares method (Paulson et al., 2013). We assessed treatment effects on overall community composition with PERMANOVA and visualized with PCoA using Bray-Curtis dissimilarities.

Differential abundance of specific families based on our treatments were tested using Linear Discriminant Analysis (LDA) Effect Size (LEfSe; Segata et al., 2011). The LEfSe allows

for statistically robust identification of features that are most likely to explain differences between experimental groups. Briefly, the method first uses a non-parametric Kruskal-Wallis sum-rank test to detect differentially abundant features across groups, followed by unpaired Wilcoxon rank-sum test, and finally LDA to estimate the effect size of each differentially abundant feature (Segata et al., 2011). LEfSe analysis was completed on taxa grouped at the family level, and significance was determined by FDR-adjusted p-value < 0.01 and log LDA score greater than 1.5. Multivariate analysis and visualization were implemented in the web-based tool MicrobiomeAnalyst (Chong et al., 2020).

3. Results

3.1 Genotype and soil treatment effects on plant growth and N uptake

Wheat yield strongly differed by year; due to severe drought in 2020, wheat yields were on average 695 kg ha^{-1}, with even lower yield in the ^{15}N microplots due to reduced moisture from soil disturbance to incorporate the residue. Therefore, the 2019-2020 wheat data was excluded from analysis, and all wheat yield and N uptake data is reported for the 2020-2021 season only. Wheat yield data from the excluded 2019-2020 season is reported in Table S3. Wheat yields from 2021 averaged 2217 kg ha^{-1}. Wheat grain yield in 2021 was 62% greater in the 0x than 5x plots (Fig. 1a), while wheat straw yield was not different between soil treatment and averaged 11,698 kg ha^{-1} (Fig. 1b). Harvest index was 54% higher in the 0x than the 5x treatment (Fig. 1c).

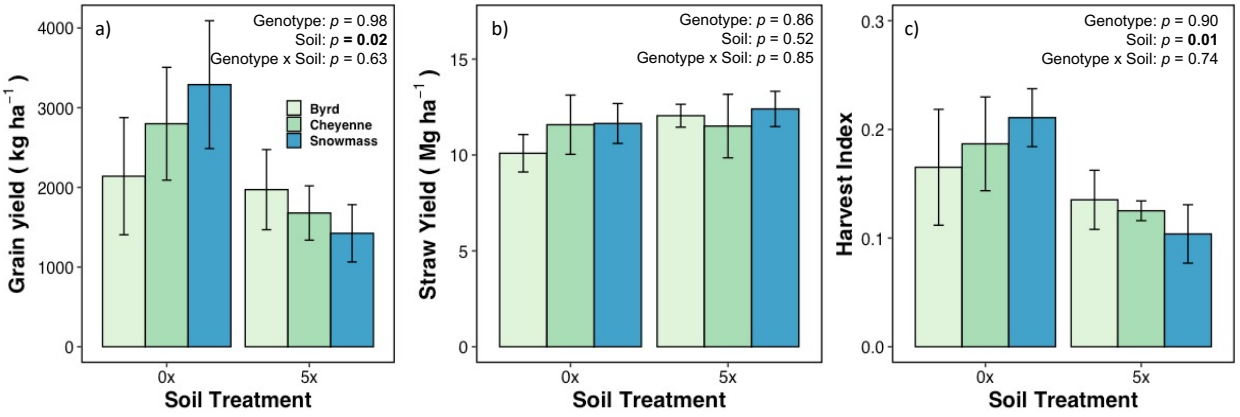

Figure 1. Wheat yield metrics from a wheat genotype and compost amendment field trial in Akron, CO. Soil treatments are biennial (every 2 years) application of beef feedlot compost at a rate of 0 t ha^{-1} (0x) or 109 t ha^{-1} (5x). Bars are colored by wheat genotype with mean ± standard error. Two-way ANOVA *p* - values are given in the top right of each panel. Data is from a single year of the trial (2020-2021 season) due to drought failure.

Total N uptake in the wheat tissue was affected by soil treatment but not by wheat genotype. While grain N concentration was the same across soil treatments (average: 2.9%), straw N concentration was 86% higher in the 5x soil treatment (1.8% vs. 0.95%). This led to more than twice as much straw N uptake in the 5x soil treatment (Table S4). However, the higher grain yield in the 0x treatment resulted in 55% more total N in the 0x (6.0 - 9.0 g N m^{-2}) grain compared to 5x grain (3.9 - 5.8 g N m^{-2}; Table S3). Overall N uptake in the wheat biomass (grain + straw) was on average 48% greater in the 5x soils, though not significant ($p = 0.12$), and there was no effect of genotype or a genotype x soil interaction (Table S4).

The uptake of cover crop-derived N was overall higher in the 0x treatment and exhibited a genotype x soil treatment interaction. Cheyenne showed the greatest plasticity in cover crop-N uptake across soil treatments, having 82% greater cover crop N uptake compared to Byrd within the 0x treatment, but then had the lowest relative cover crop-N uptake in the 5x treatment, 41% less than Byrd (Fig 2a). Snowmass also had almost half the cover crop-N uptake in the 5x treatment relative to the 0x treatments, but Byrd was consistent with no change across the different compost treatments. Across all samples, the wheat took up an average of 4.9 kg of cover crop N per ha, 13% (range: 7%-22%) of the added residue N (Fig. 2a).

The relative concentration of wheat tissue N derived from the added cover crop residue was consistent with trends in total residue N uptake (Fig. 2b). Plants in the 0x soil treatment had 3.0 – 4.4% of their grain N derived from the added cover crop residue, but this was reduced to 1.1-1.9% in the 5x soils (Fig. 2b). Enrichment was on average 0.54 atm% ^{15}N in grain samples and 0.55 atm% ^{15}N in straw. This translated to an average of 2.4% of grain N and 2.6% of the

Figure 2. Total uptake (a) and relative fraction (b) of cover-crop residue (CC) derived N in wheat biomass tissue in different winter wheat genotypes and compost amendment treatments in field trial in Akron, CO. Soil treatments are biennial (every 2 years) application of beef feedlot compost at a rate of 0 t ha-1 (0x) or 109 t ha-1 (5x). Bars are colored by wheat genotype with mean ± standard error. Two-way ANOVA p - values are given in the top right. Data is from a single year of the trial (2020-2021 season) due to drought failure in year 1.

straw N being derived from the cover crop.

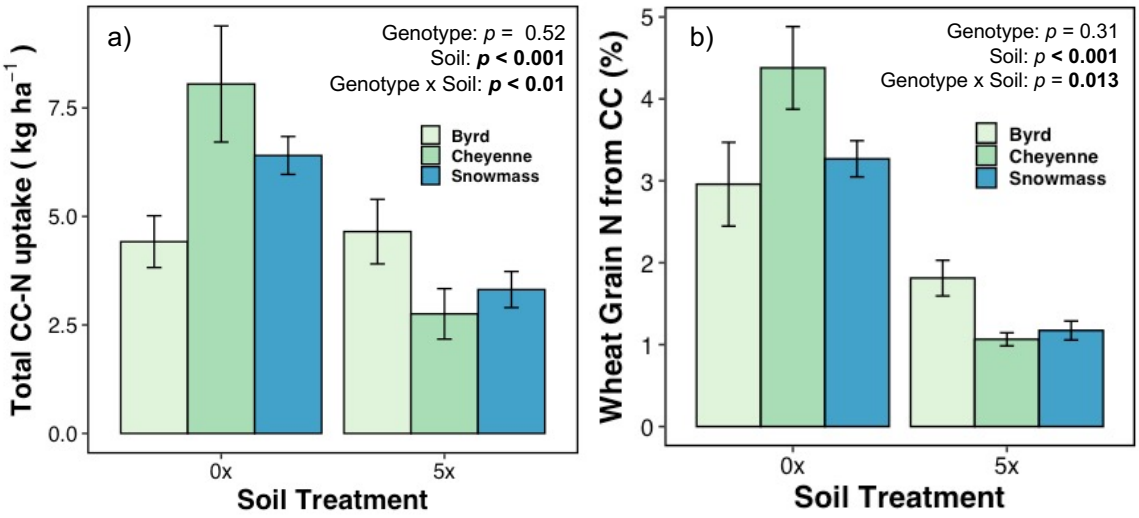

3.2 Enzyme activities

Enzyme activities responded strongly to soil treatment but not to wheat genotype. For all enzymes assayed, activities in the 5x soil were greater than the 0x soil except for PHOS, which had higher activity in the 0x soil (Table 2). Enzyme activity was 40-48% higher at the second sampling timepoint (heading/flowering) in all enzymes except the two aminopeptidases, LAP and TAP (Table 2). In all enzymes except TAP, activity was higher in the second, wetter season (2019-2020; Table 2). Both years of data were included in enzyme analysis, as well as for inorganic N and microbiome analyses below, as these samples were collected from the main genotype plot earlier in the season before severe water limitation, and patterns were aligned with the 2021 data.

3.3 Soil N and water

Soil nitrate and ammonium concentrations at tillering and heading showed differences based on soil treatment, but there was no effect of wheat genotype on either form of inorganic N. Both ammonium and nitrate were higher in the 5x soil (Table 3). We did not observe a relationship between enzyme activity and inorganic N levels after accounting for the large effect of compost addition (data not shown). Sampling timepoint effects varied by N form and year; in 2020, ammonium levels were higher at tillering with no change in nitrate, while in 2021, nitrate levels were higher at tillering with no change in ammonium (Table 3).

Gravimetric water content (GWC) in the top 30 cm of soil decreased over the course of the growing season. GWC in the surface soil was ~10-20% higher the 5x rhizosphere soil samples during the growing season (tillering and heading), but the differences faded by the harvest sampling (Table S6).

3.4 Rhizosphere microbiome analysis

Following initial feature filtering, we observed 8,640 distinct bacterial/archaeal features and 1,985 fungal features across bother years. The total number of features in a single sample ranged from 21, 177 to 151, 505, and we did not have to exclude any samples due to low read counts. Rhizosphere bacterial communities were dominated by Actinobacteria and Proteobacteria, and Ascomycota was overwhelmingly dominant in the fungal community (Fig. S3, S4).

Shannon diversity of both bacterial/archaeal and fungal taxa were 2.6 and 7.6% lower, respectively, in the 5x compost treatments than the 0x treatments, and there was a marginally significant genotype effect on fungal diversity (Table S5). Specifically, the historic genotype Cheyenne had 7.3% higher fungal diversity (Shannon) compared to Byrd (Table S5). Across both years, all three metrics of bacterial diversity were greater at the later heading timepoint, while only fungal richness showed an increase at heading. The effect of year was different for fungi vs. bacteria, with bacterial diversity and richness being greater in 2020, but fungal diversity higher in 2021.

Both bacterial and fungal communities showed high separation due to soil treatment (Fig. 3a,d), but there were no differences based on genotype (Fig. 3b,e) or sampling timepoint (Fig. 3c,e)). LEfSe analysis identified a suite of bacterial and fungal families that contributed to the soil treatment differences observed (Fig. S1, Fig. S2). For bacterial families, we found that Rubrobacteriaceae and Sphingomonadaceae were strongly associated with the 0x soils, while Planococcaceae, Devosiaceae, Rhizobiaceae, and Pseudomonadaceae were associated with 5x soil. At the phylum level, Proteobacteria, Bacteriodetes and Firmicutes were most associated with 5x soil, while Actinobacteria were more abundant in the 0x soil (Fig. S2). For fungi, Chaetomiaceae and Sporomiaceae were associated with 5x soil, and Aspergillaceae and Lasiosphaeriaceae with the 0x soil (Fig. S1). No bacterial or fungal taxa were identified as contributing significantly to group separation by wheat genotype according to LEfSe analysis.

Due to additional filtering of rare and low-variability features, 1862 bacterial and 302 fungal features were ultimately used in multivariate analysis.

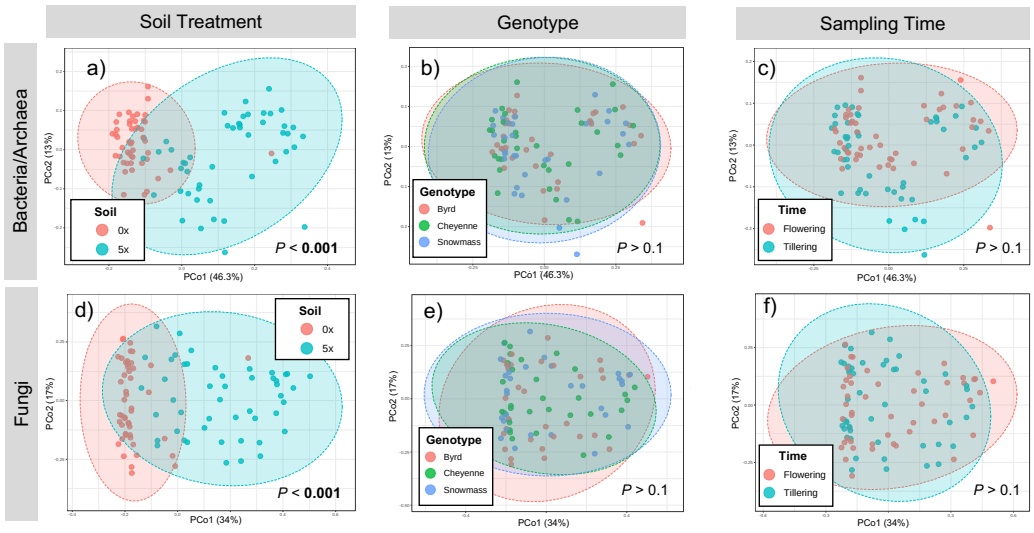

Figure 3. Principle Coordinate Analysis (PCoA) of winter wheat rhizosphere communities based on 16S (top) and ITS (bottom) amplicon sequencing. Samples are colored based on long-term compost amendment (left), wheat genotype (center), or sampling timepoint (right). PERMANOVA p - values are indicated in the bottom right corner for the significance of the groupings. Figure includes data from both growing seasons.

4. Discussion

4.1 Yield response

Treatment effects on wheat grain yield were different than expected, and appeared to be strongly influenced by precipitation patterns. We found higher grain yield in the no-compost plots, though overall higher biomass production in the 5x treatment. This is despite the typical indicators of N availability and N cycling being greater in the 5x treatment, which was expected due to nutrient addition (Table 2, Table 3). The unexpected yield results, whereby grain yield was higher in the 0x treatment, was likely explained by the seasonal rainfall patterns experienced in 2021.

We suspect that relatively high rainfall in the spring and early summer supported strong vegetative growth, especially in the 5x treatment with higher overall nutrient availability. However, this growth eventually led to water limitation in June and July when precipitation was below average (Table S2), such that the larger plants in the 5x plots were transpiring more and ran out of water during grain filling, resulting in low grain production for this treatment and a lower harvest index (Fig. 1c). We suspect that water limitation also impeded N translocation to the grain, resulting in high N concentration in the biomass of the 5x wheat, though not reflected

in the grain. Despite the higher nutrients in the 5x soil, previous research from these plots similarly found no significant difference in wheat biomass between the compost amendment treatments, though greater N concentration in wheat tissues (Calderón et al., 2018).

We did not observe genotype differences in grain or straw yield, despite the historic genotype, Cheyenne, being a tall variety and not possessing the semi-dwarfing allele common in many modern cultivars, including the two current genotypes included in the study (Table 1). This result further highlights the importance of environmental effects that may obscure even well-established genetic differences.

4.2 Differential genotype uptake patterns of residue N

Our results suggest that wheat genotypes with different nutrient acquisition strategies (i.e., "cooperative" vs. competitive") have varying ability to access cover crop N depending on the soil status. In contrast to our hypothesis, the older and high-exudate genotypes were not more successful in the high SOM (5x) environment; instead, it appears that the high SOM context provided the background microbial activity necessary to drive the turnover of residue N, supported by increased enzyme activity and extractable N in the 5x treatment (Table 2, 3), allowing other root traits, like drought tolerance, to determine relative success at organic nutrient acquisition.

Genotypic variation in belowground allocation has been previously observed for different types of wheat (Iannucci et al., 2021; Kelly et al., 2022b) which lends evidence for different resource acquisition strategies, even within a species. Different acquisition strategies may include the "collaborative" strategy, where high levels of exudation support microbial activity and encourages nutrient mineralization proximate to the root zone (Henneron et al., 2020). In contrast, a more competitive strategy dedicates resources to root structures for better soil exploration and more direct uptake of nutrients instead of promoting microbial partnerships (Bergmann et al., 2020; Wen et al., 2019, 2022). Though we did not measure root exudation in this study directly, the genotypes used in this study have been previously shown to exhibit both high exudate (Snowmass) and low-exudation (Byrd) strategies, while the historic germplasm Cheyenne had intermediate exudation but may have other differences in root traits from its distinct lineage (Kelly et al., 2022b). Our findings suggest that long-term compost amendment, which alters the microbial community (Fig. 3) and increases enzyme activity and nutrient

availability (Table 2, Table 3), likely influences the relative success of these different strategies, and that water limitation further increases the complexity of plant-soil-microbe interactions.

Cheyenne and Snowmass were more successful than Byrd at taking up residue-derived N in the 0x soil (Fig. 1), which we suspect was due to higher exudation rates (Kelly et al., 2022b), resulting in greater microbial mineralization of organic N, in this more C- and N-limited soil. Both Cheyenne and Snowmass have been reported to be drought susceptible due to shallower root systems (Kim et al., 2016), and so likely concentrated more of their roots near the surface in proximity to the added N-rich residue. Importantly, Snowmass has also been shown to have high levels of root exudation, and has more recently been shown to recruit specific microbial taxa, compared to Byrd (Kelly et al., 2022b, 2022a). We suspect that in the 0x soils, which have lower native SOM and biological activity, microbes were in a C-limited state, and thus more responsive to exudate additions. Previous work has found that soil condition affects the microbial mineralization response to exudation regarding litter decomposition (Tian et al., 2019). Though we did not measure N mineralization rates directly in this study, we assume that residue N uptake provides a practical estimate of plant-available mineralized N. Our results indicate that, under C and N limitation in degraded agricultural soils, genotypes with greater exudation, i.e. more "collaborative", have greater access to organic N sources than in the high SOM soil, and that the success of different nutrient acquisition strategies are dependent on the soil characteristics.

While we did not observe genotype differences in enzyme activity (Table S3), we note that our samples were collected outside of the residue-addition microplots and so rhizosphere responses to the added residue were not specifically tested. Root exudation has been shown to stimulate N cycling enzyme activity and N availability in field and greenhouse settings, as microbes release enzymes to alleviate N limitation (Hamilton & Frank, 2001; Kelly et al., 2022b; Zhu et al., 2014). While a previous greenhouse experiment found high exudation to impede short-term residue N uptake in low-SOM soil under greenhouse conditions (Kelly et al., 2022a), field conditions and a longer growing season create a different nutrient dynamic. Specifically, the longer growing time tested here allows for greater microbial turnover of added residues, allowing plants to access previously-immobilized microbial N (Kuzyakov & Xu, 2013). This suggests that it is important to consider full-season biogeochemical cycling when translating greenhouse work to the field.

In the compost-amended soil, wheat genotype performance with regard to residue N uptake showed a different trend. While Byrd took up the lowest residue-N in the 0x soil, it surpassed the other genotypes in the 5x soil (Fig. 1). In the 5x soil, high levels of SOM and microbial activity (i.e. enzymes; Table 2) likely muted or diluted the exudate effect. Indeed, exudate stimulation of litter decomposition was reduced in high-SOM soil (Tian et al., 2019). In the high-SOM soils of this experiment, therefore, water became a more important factor for success, and thus drought tolerance a key genotype trait. Unlike the other genotypes, Byrd has been reported to be drought-tolerant with a deep-rooting morphology (Becker et al., 2016). Greater access to water deeper in the soil profile may have allowed Byrd to continue to grow and access residue N throughout the dry summer season. While not significantly different, we note that Byrd had on average the highest grain yield and harvest index in the 5x treatments (Fig. 1a,c), suggesting that it may have been able to maintain growth later in the season when conditions became especially dry, with relatively less vegetative growth to maintain.

Together, our data suggests that in higher SOM environments, exudation may be less important in mobilizing organic N sources, increasing the importance other limiting resources (i.e., water) in nutrient acquisition (Fig. 4). Thus, while less successful at accessing residue N in low-SOM and low-activity soil, we suspect that greater drought tolerance within the microbially-active 5x soil was a key driver for Byrd in the uptake of residue-derived N. Our results highlight the importance of the environmental context in elevating the relative importance of genotype traits and different nutrient acquisition strategies, as high levels of soil health indicators may

effectively drive nutrient mineralization without plant investment.

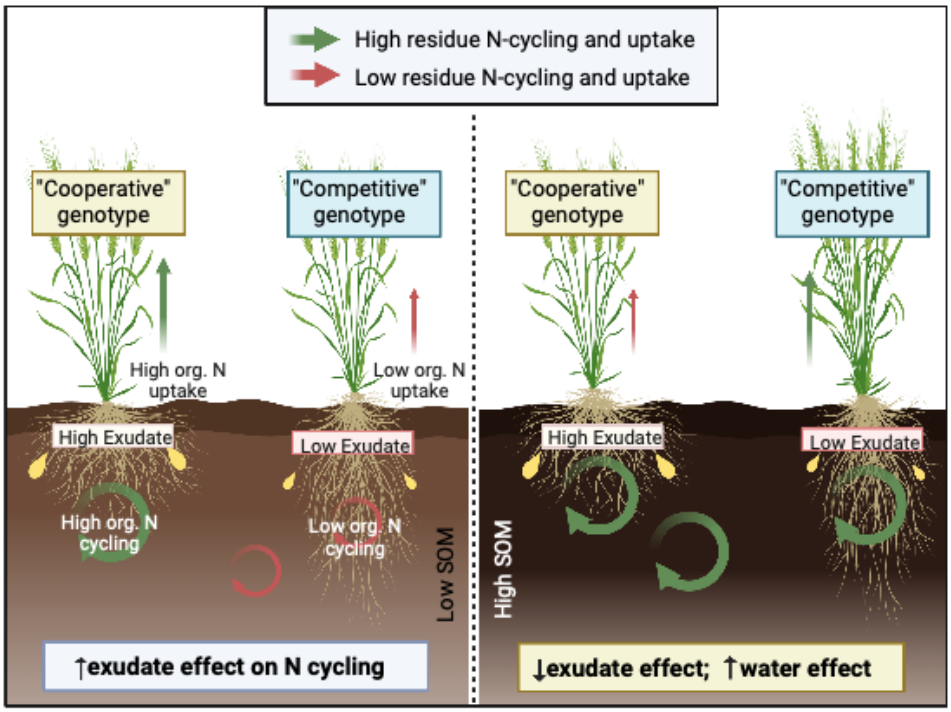

Figure 4. Summary figure of interactive effects of soil management legacy and genotype on nitrogen (N) cycling and uptake. Size of blue arrows indicates relative rate of N cycling and plant uptake based on our research findings.

4.3 Microbial community

Microbial community structure and function was strongly affected by compost amendment, but we did not observe any differences due to wheat genotype or sampling time (Fig 3; Table 2). Both C and N cycling enzymes were elevated in soil with long-term compost amendment, which was likely due to higher levels of complex C and N substrates (Bowles et al., 2014). Phosphatase activity (PHOS) was lower in the 5x soils, reflecting the well-documented inverse relationship between available P and phosphatase activity (Kitayama, 2013; Sinsabaugh et al., 2008). We were unable to observe genotype differences in enzyme activity, which could be partly due assay limitations in sensitivity and field variability (Trasar-Cepeda et al., 2000).

The higher Shannon diversity in the 0x treatment suggests that a lower nutrient environment created more niche opportunities and less dominance by copiotrophic taxa (Fierer et al., 2007). Lower microbial diversity has been reported for high-nutrient soil environments like the rhizosphere and soils with organic additions (Brisson et al., 2019), though others have found

increased bacterial diversity with compost additions (Mickan et al., 2018; Zhen et al., 2014). Fungal diversity was highest in the historic genotype Cheyenne, which echoes previous work showing that historic varieties of wheat had greater reliance mycorrhizal association than modern varieties (Hetrick et al., 1993).

We did not identify any bacterial or fungal taxa that were differentially abundant across genotypes, which suggests that genotype-level variation in rhizosphere community selection were overwhelmed by the strong environmental differences between the 0x and 5x compost soils. We note that some weed presence may have obscured genotype effects, especially in 2020 before herbicide use was implemented. Similar to our findings, a study of different wheat genotypes cultivated with different farm management and drought treatments found that drought and farming system explained significant variability in microbial communities, but genotype effects were not apparent (Breitkreuz et al., 2021). Even under similar conditions, genotype effects on rhizosphere communities are often subtle and difficult to detect (Kelly et al., 2022b). Studies comparing rhizosphere microbiomes of different genotypes for a variety of crops have suggested that genotype differences can influence microbiome assembly, but that different environmental conditions (soil type, nutrient management) have a larger effect (Schmidt et al., 2020).

Acidobacteria, which were highly indicative of the 0x soil and have species known to be ecological "stress tolerators", were found to be the most abundant phylum in undisturbed natural soils across a range of ecosystems (Fierer, 2017). The higher-nutrient environment of the 5x soil likely favored more competitive taxa, including members of Pseudomonas which were found to be highly abundant (Fig. S1a). Also common in the 5x soils was the Rhizobiaceae, which includes many species of Rhizobia, common soil and plant-associated bacteria and include N-fixers as well as plant pathogens (Alves, 2013).

Conclusions

As agroecosystems evolve to provide additional ecosystem services like nutrient retention and C storage, there will be a greater reliance on organic nutrient provision. It has been hypothesized that unintended consequences of plant breeding on rhizosphere interactions maybe cause disadvantages to modern crops in a soils with fewer synthetic inputs. We found that soils with high levels of SOM better support nutrient cycling activities, regardless of crop genotype. In

addition, stronger rhizosphere partnerships via exudation may be more important in degraded, C-depleted soils. Importantly, we suspect a been a trade-off between microbial stimulation via exudation and deep rooting morphology led to genotype differences under water limitation. Therefore, it is critical to consider the coupling of biological activity, nutrient cycling and water availability when breeding and selecting crop traits for agroecosystems in a changing environment.

Acknowledgements

The authors would like to acknowledge the help of Brandon Peterson, Cody Hardy, and David Poss at the USDA-ARS in Akron for their help with experimental implementation and data collection. The authors also thank Carolita Landers for help with sample processing and Kristen Otto for logistical support in amplicon sequencing. We also thank the anonymous reviewers who provided valuable feedback on earlier versions of this manuscript. This project was funded by the USDA National Institute of Food and Agriculture (Award No. 2018-67013-27398). Work at LLNL was performed under the auspices of the US Department of Energy at Lawrence Livermore National Laboratory under Contract DE-AC52-07NA27344.

Data Availability

All sequencing data is available online in the NCBI SRA databased under project and submission PRJNA735275 SUB11809024. Biogeochemical data will be uploaded to an online repository upon acceptance of this manuscript.

563 Literature Cited
564
565 Abarenkov, K., Zirk, A., Piirmann, T., Pöhönen, R., Ivanov, F., Nilsson, R. H., & Kõljalg, U.
566 (2020). UNITE QIIME release for Fungi. Version 04.02.2020. *UNITE Community*.
567 https://doi.org/https://doi.org/10.15156/BIO/786385
568 Alves. (2013). *The Family Rhizobiaceae*. Springer. https://doi.org/10.1007/978-3-642-30197-
569 1_297
570 Bates, D., Maechler, M., Bolker, B., & Walker, S. (2015). Fitting Linear Mixed-Effects Models
571 Using lme4. *Journal of Statistical Software*, *67*(1), 1–48.
572 https://doi.org/10.18637/jss.v067.i01
573 Becker, S. R., Byrne, P. F., Reid, S. D., Bauerle, W. L., McKay, J. K., & Haley, S. D. (2016).
574 Root traits contributing to drought tolerance of synthetic hexaploid wheat in a greenhouse
575 study. *Euphytica*, *207*(1), 213–224. https://doi.org/10.1007/s10681-015-1574-1
576 Bergmann, J., Weigelt, A., van der Plas, F., Laughlin, D. C., Kuyper, T. W., Guerrero-Ramirez,
577 N., Valverde-Barrantes, O. J., Bruelheide, H., Freschet, G. T., Iversen, C. M., Kattge, J.,
578 Mccormack, M. L., Meier, I. C., Rillig, M. C., Roumet, C., Semchenko, M., Sweeney, C.
579 J., van Ruijven, J., York, L. M., & Mommer, L. (2020). The fungal collaboration gradient
580 dominates the root economics space in plants. *Sci. Adv*, *6*. https://www.science.org
581 Bokulich, N. A., Kaehler, B. D., Rideout, J. R., Dillon, M., Bolyen, E., Knight, R., Huttley, G.
582 A., & Gregory Caporaso, J. (2018). Optimizing taxonomic classification of marker-gene
583 amplicon sequences with QIIME 2's q2-feature-classifier plugin. *Microbiome*, *6*(1), 1–
584 17. https://doi.org/10.1186/s40168-018-0470-z
585 Bolyen, E., Rideout, J. R., Dillon, M. R., Bokulich, N. A., Abnet, C. C., Al-Ghalith, G. A.,
586 Alexander, H., Alm, E. J., Arumugam, M., Asnicar, F., Bai, Y., Bisanz, J. E., Bittinger,
587 K., Brejnrod, A., Brislawn, C. J., Brown, C. T., Callahan, B. J., Caraballo-Rodríguez, A.
588 M., Chase, J., … Caporaso, J. G. (2019). Reproducible, interactive, scalable and
589 extensible microbiome data science using QIIME 2. *Nature Biotechnology*, *37*(8), 852–
590 857. https://doi.org/10.1038/s41587-019-0209-9
591 Bowles, T. M., Acosta-Martínez, V., Calderón, F., & Jackson, L. E. (2014). Soil enzyme
592 activities, microbial communities, and carbon and nitrogen availability in organic
593 agroecosystems across an intensively-managed agricultural landscape. *Soil Biology and*
594 *Biochemistry*, *68*, 252–262. https://doi.org/10.1016/j.soilbio.2013.10.004

595 Breitkreuz, C., Herzig, L., Buscot, F., Reitz, T., & Tarkka, M. (2021). Interactions between soil
596 properties, agricultural management and cultivar type drive structural and functional
597 adaptations of the wheat rhizosphere microbiome to drought. *Environmental*
598 *Microbiology*, *23*(10), 5866–5882. https://doi.org/10.1111/1462-2920.15607
599 Brisson, V. L., Schmidt, J. E., Northen, T. R., Vogel, J. P., & Gaudin, A. C. M. (2019). Impacts
600 of Maize Domestication and Breeding on Rhizosphere Microbial Community
601 Recruitment from a Nutrient Depleted Agricultural Soil. *Scientific Reports*, *9*(1), 1–14.
602 https://doi.org/10.1038/s41598-019-52148-y
603 Calderón, F. J., Vigil, M. F., & Benjamin, J. (2018). Compost Input Effect on Dryland Wheat
604 and Forage Yields and Soil Quality. *Pedosphere*, *28*(3), 451–462.
605 https://doi.org/10.1016/S1002-0160(17)60368-0
606 Callahan, B. J., Mcmurdie, P. J., Rosen, M. J., Han, A. W., Johnson, A. J. A., & Holmes, S. P.
607 (2016). DADA2: High-resolution sample inference from Illumina amplicon data. *Nature*
608 *Methods*, *13*(7), 581–583. https://doi.org/10.1038/nmeth.3869
609 Caporaso, J. G., Lauber, C. L., Walters, W. A., Berg-Lyons, D., Lozupone, C. A., Turnbaugh, P.
610 J., Fierer, N., & Knight, R. (2011). Global patterns of 16S rRNA diversity at a depth of
611 millions of sequences per sample. *Proceedings of the National Academy of Sciences of*
612 *the United States of America*, *108*(SUPPL. 1), 4516–4522.
613 https://doi.org/10.1073/pnas.1000080107
614 Chong, J., Liu, P., Zhou, G., & Xia, J. (2020). Using MicrobiomeAnalyst for comprehensive
615 statistical, functional, and meta-analysis of microbiome data. *Nature Protocols*, *15*(3),
616 799–821. https://doi.org/10.1038/s41596-019-0264-1
617 Fierer, N. (2017). Embracing the unknown: disentangling the complexities of the soil
618 microbiome. *Nature Reviews Microbiology*, *15*(10), 579–590.
619 https://doi.org/10.1038/nrmicro.2017.87
620 Fierer, N., Bradford, M. A., & Jackson, R. B. (2007). Toward an ecological classification of soil
621 bacteria. *Ecology*, *88*(6), 1354–1364. https://doi.org/10.1890/05-1839
622 Fitzpatrick, C. R., Copeland, J., Wang, P. W., Guttman, D. S., Kotanen, P. M., & Johnson, M. T.
623 J. (2018). Assembly and ecological function of the root microbiome across angiosperm
624 plant species. *Proceedings of the National Academy of Sciences*, 201717617.
625 https://doi.org/10.1073/pnas.1717617115

Foulkes, M. J., Hawkesford, M. J., Barraclough, P. B., Holdsworth, M. J., Kerr, S., Kightley, S., & Shewry, P. R. (2009). Identifying traits to improve the nitrogen economy of wheat: Recent advances and future prospects. In *Field Crops Research* (Vol. 114, Issue 3, pp. 329–342). https://doi.org/10.1016/j.fcr.2009.09.005

Gan, D., Zeng, H., & Zhu, B. (2022). The rhizosphere effect on soil gross nitrogen mineralization: A meta-analysis. *Soil Ecology Letters*, *4*(2), 144–154. https://doi.org/10.1007/s42832-021-0098-y

German, D. P., Weintraub, M. N., Grandy, A. S., Lauber, C. L., Rinkes, Z. L., & Allison, S. D. (2011). Optimization of hydrolytic and oxidative enzyme methods for ecosystem studies. *Soil Biology and Biochemistry*, *43*(7), 1387–1397. https://doi.org/10.1016/j.soilbio.2011.03.017

Haley, S. D., Johnson, J. J., Peairs, F. B., Stromberger, J. A., Heaton, E. E., Seifert, S. A., Kottke, R. A., Rudolph, J. B., Martin, T. J., Bai, G., Chen, X., Bowden, R. L., Jin, Y., Kolmer, J. A., Seifers, D. L., Chen, M.-S., & Seabourn, B. W. (2011). Registration of 'Snowmass' Wheat. *Journal of Plant Registrations*, *5*(1), 87–90. https://doi.org/10.3198/JPR2010.03.0175CRC

Haley, S. D., Johnson, J. J., Peairs, F. B., Stromberger, J. A., Hudson, E. E., Seifert, S. A., Kottke, R. A., Valdez, V. A., Rudolph, J. B., Bai, G., Chen, X., Bowden, R. L., Jin, Y., Kolmer, J. A., Chen, M.-S., & Seabourn, B. W. (2012). Registration of 'Byrd' Wheat. *Journal of Plant Registrations*, *6*(3), 302–305. https://doi.org/10.3198/jpr2011.12.0672crc

Hamilton, E. W., & Frank, D. A. (2001). Can plants stimulate soil microbes and their own nutrient supply? Evidence from a grazing tolerant grass. *Ecology*, *82*(9), 2397–2402. https://doi.org/10.1890/0012-9658(2001)082[2397:CPSSMA]2.0.CO;2

Henneron, L., Kardol, P., Wardle, D. A., Cros, C., & Fontaine, S. (2020). Rhizosphere control of soil nitrogen cycling: a key component of plant economic strategies. *New Phytologist*, *228*(4), 1269–1282. https://doi.org/10.1111/nph.16760

Hetrick, B. A. D., Wilson, G. W. T., & Cox, T. S. (1993). Mycorrhizal dependence of modern wheat cultivars and ancestors: a synthesis. *Canadian Journal of Botany*, *71*(3), 512–518. https://doi.org/10.1139/b93-056

Hoagland, D. R., & Arnon, D. I. (1950). The water-culture method for growing plants without soil. *Circular: California Agricultural Experiment Station*, *347*(2).

Huo, C., Luo, Y., & Cheng, W. (2017). Rhizosphere priming effect: A meta-analysis. *Soil Biology and Biochemistry*, *111*, 78–84. https://doi.org/10.1016/j.soilbio.2017.04.003

Iannucci, A., Canfora, L., Nigro, F., de Vita, P., & Beleggia, R. (2021). Relationships between root morphology, root exudate compounds and rhizosphere microbial community in durum wheat. *Applied Soil Ecology*, *158*(February 2020). https://doi.org/10.1016/j.apsoil.2020.103781

Janzen, H. H., Janzen, D. W., & Gregorich, E. G. (2021). The 'soil health' metaphor: Illuminating or illusory? *Soil Biology and Biochemistry*, *159*, 108167. https://doi.org/10.1016/J.SOILBIO.2021.108167

Kelly, C., Haddix, M. L., Byrne, P. F., Cotrufo, M. F., Schipanski, M. E., Kallenbach, C. M., Wallenstein, M. D., & Fonte, S. J. (2022a). Long-term compost amendment modulates wheat genotype differences in belowground carbon allocation, microbial rhizosphere recruitment and nitrogen acquisition. *Soil Biology and Biochemistry*, *172*, 108768. https://doi.org/10.1016/j.soilbio.2022.108768

Kelly, C., Haddix, M. L., Byrne, P. F., Cotrufo, M. F., Schipanski, M., Kallenbach, C. M., Wallenstein, M. D., & Fonte, S. J. (2022b). Divergent belowground carbon allocation patterns of winter wheat shape rhizosphere microbial communities and nitrogen cycling activities. *Soil Biology and Biochemistry*, *165*, 108518. https://doi.org/10.1016/j.soilbio.2021.108518

Kelly, C., Schipanski, M. E., Tucker, A., Trujillo, W., Obour, A., Holman, J. D., Johnson, S. K., Brummer, J. E., Haag, L., & Fonte, S. J. (2021). Dryland cover crop soil health benefits are maintained with grazing in the U.S. High and Central Plains. *Agriculture, Ecosystems & Environment*, *313*, 107358. https://doi.org/10.1016/j.agee.2021.107358

Kim, K. S., Anderson, J. D., Newell, M. A., Grogan, S. M., Byrne, P. F., Baenziger, P. S., & Butler, T. J. (2016). Genetic diversity of great plains hard winter wheat germplasm for forage. *Crop Science*, *56*(5), 2297–2305. https://doi.org/10.2135/CROPSCI2015.08.0519

Kitayama, K. (2013). The activities of soil and root acid phosphatase in the nine tropical rain forests that differ in phosphorus availability on Mount Kinabalu, Borneo. *Plant and Soil*, *367*(1–2), 215–224. https://doi.org/10.1007/s11104-013-1624-1

687 Kuznetsova, A., Brockhoff, P. B., & Christensen, R. H. B. (2017). lmerTest Package: Tests in
688 linear Mixed Effects Models. *Journal of Statistical Software*, *82*(13), 1–26.
689 https://doi.org/10.18637/jss.v082.i13}
690 Kuzyakov, Y., & Xu, X. (2013). Competition between roots and microorganisms for nitrogen:
691 mechanisms and ecological relevance. *New Phytologist*, *198*(3), 656–669.
692 https://doi.org/10.1111/nph.12235
693 Liu, J., Calderón, F. J., & Fonte, S. J. (2021). Compost inputs, cropping system, and rotation
694 phase drive aggregate-associated carbon. *Soil Science Society of America Journal*, *85*(3),
695 829–846. https://doi.org/10.1002/saj2.20252
696 Mendes, L. W., Raaijmakers, J. M., de Hollander, M., Mendes, R., & Tsai, S. M. (2018).
697 Influence of resistance breeding in common bean on rhizosphere microbiome
698 composition and function. *ISME Journal*, *12*(1), 212–224.
699 https://doi.org/10.1038/ismej.2017.158
700 Mickan, B. S., Abbott, L. K., Fan, J., Hart, M. M., Siddique, K. H. M., Solaiman, Z. M., &
701 Jenkins, S. N. (2018). Application of compost and clay under water-stressed conditions
702 influences functional diversity of rhizosphere bacteria. *Biology and Fertility of Soils*,
703 *54*(1), 55–70. https://doi.org/10.1007/s00374-017-1238-5
704 Paulson, J. N., Stine, O. C., Bravo, H. C., & Pop, M. (2013). Differential abundance analysis for
705 microbial marker-gene surveys. *Nature Methods*, *10*(12), 1200–1202.
706 https://doi.org/10.1038/nmeth.2658
707 Pérez-Jaramillo, J. E., Mendes, R., & Raaijmakers, J. M. (2016). Impact of plant domestication
708 on rhizosphere microbiome assembly and functions. *Plant Molecular Biology*, *90*(6),
709 635–644. https://doi.org/10.1007/s11103-015-0337-7
710 Qu, Q., Zhang, Z., Peijnenburg, W. J. G. M., Liu, W., Lu, T., Hu, B., Chen, J., Chen, J., Lin, Z.,
711 & Qian, H. (2020). Rhizosphere Microbiome Assembly and Its Impact on Plant Growth.
712 In *Journal of Agricultural and Food Chemistry* (Vol. 68, Issue 18, pp. 5024–5038).
713 American Chemical Society. https://doi.org/10.1021/acs.jafc.0c00073
714 Quast, C., Pruesse, E., Yilmaz, P., Gerken, J., Schweer, T., Yarza, P., Peplies, J., & Glöckner, F.
715 O. (2013). The SILVA ribosomal RNA gene database project: Improved data processing
716 and web-based tools. *Nucleic Acids Research*, *41*(D1), 590–596.
717 https://doi.org/10.1093/nar/gks1219

718 R Core Team. (2020). *R: A Language and Environment for Statistical Computing*. https://www.r-
719 project.org/
720 Reich, P. B. (2014). The world-wide "fast-slow" plant economics spectrum: A traits manifesto.
721 *Journal of Ecology*, *102*(2), 275–301. https://doi.org/10.1111/1365-2745.12211
722 Sánchez-Cañizares, C., Jorrín, B., Poole, P. S., & Tkacz, A. (2017). Understanding the holobiont:
723 the interdependence of plants and their microbiome. *Current Opinion in Microbiology*,
724 *38*, 188–196. https://doi.org/10.1016/j.mib.2017.07.001
725 Schmidt, J. E., Bowles, T. M., & Gaudin, A. C. M. (2016). Using Ancient Traits to Convert Soil
726 Health into Crop Yield: Impact of Selection on Maize Root and Rhizosphere Function.
727 *Frontiers in Plant Science*, *7*(March), 1–11. https://doi.org/10.3389/fpls.2016.00373
728 Schmidt, J. E., Rodrigues, J. L. M., Brisson, V. L., Kent, A., & Gaudin, A. C. M. (2020). Impacts
729 of directed evolution and soil management legacy on the maize rhizobiome. *Soil Biology*
730 *and Biochemistry*, *145*, 107794. https://doi.org/10.1016/j.soilbio.2020.107794
731 Segata, N., Izard, J., Waldron, L., Gevers, D., Miropolsky, L., Garrett, W. S., & Huttenhower, C.
732 (2011). Metagenomic biomarker discovery and explanation. *Genome Biology*, *12*(6).
733 https://doi.org/10.1186/gb-2011-12-6-r60
734 Sinsabaugh, R. L., Lauber, C. L., Weintraub, M. N., Ahmed, B., Allison, S. D., Crenshaw, C.,
735 Contosta, A. R., Cusack, D., Frey, S., Gallo, M. E., Gartner, T. B., Hobbie, S. E.,
736 Holland, K., Keeler, B. L., Powers, J. S., Stursova, M., Takacs-Vesbach, C., Waldrop, M.
737 P., Wallenstein, M. D., … Zeglin, L. H. (2008). Stoichiometry of soil enzyme activity at
738 global scale. *Ecology Letters*, *11*(11), 1252–1264. https://doi.org/10.1111/j.1461-
739 0248.2008.01245.x
740 Six, J., Bossuyt, H., Degryze, S., & Denef, K. (2004). A history of research on the link between
741 (micro)aggregates, soil biota, and soil organic matter dynamics. *Soil and Tillage*
742 *Research*, *79*(1), 7–31. https://doi.org/10.1016/j.still.2004.03.008
743 Tian, K., Kong, X., Yuan, L., Lin, H., He, Z., Yao, B., Ji, Y., Yang, J., Sun, S., & Tian, X.
744 (2019). Priming effect of litter mineralization: the role of root exudate depends on its
745 interactions with litter quality and soil condition. *Plant and Soil*, *440*(1–2), 457–471.
746 https://doi.org/10.1007/s11104-019-04070-5
747 Tkacz, A., Pini, F., Turner, T. R., Bestion, E., Simmonds, J., Howell, P., Greenland, A., Cheema,
748 J., Emms, D. M., Uauy, C., & Poole, P. S. (2020). Agricultural Selection of Wheat Has

Been Shaped by Plant-Microbe Interactions. *Frontiers in Microbiology*, *11*(February), 0–9. https://doi.org/10.3389/fmicb.2020.00132

Tonitto, C., David, M. B., & Drinkwater, L. E. (2006). Replacing bare fallows with cover crops in fertilizer-intensive cropping systems: A meta-analysis of crop yield and N dynamics. *Agriculture, Ecosystems and Environment*, *112*(1), 58–72. https://doi.org/10.1016/j.agee.2005.07.003

Trasar-Cepeda, C., Leirós, M. C., Seoane, S., & Gil-Sotres, F. (2000). Limitations of soil enzymes as indicators of soil pollution. *Soil Biology and Biochemistry*, *32*(13), 1867–1875. https://doi.org/10.1016/S0038-0717(00)00160-7

Wen, Z., Li, H., Shen, Q., Tang, X., Xiong, C., Li, H., Pang, J., Ryan, M. H., Lambers, H., & Shen, J. (2019). Tradeoffs among root morphology, exudation and mycorrhizal symbioses for phosphorus-acquisition strategies of 16 crop species. *New Phytologist*, *223*(2), 882–895. https://doi.org/10.1111/nph.15833

Wen, Z., White, P. J., Shen, J., & Lambers, H. (2022). Linking root exudation to belowground economic traits for resource acquisition. *New Phytologist*, *233*(4), 1620–1635. https://doi.org/10.1111/nph.17854

White, T. J., Bruns, T., Lee, S., & Taylor, J. (1990). Amplification and direct sequenceing of fungal ribosobal RNA genes for phylogenetics. In M. A. Innis, D. H. Gelfand, J. J. Sninsky, & T. J. White (Eds.), *PCR Protocols: a Guide to Methods and Applications* (pp. 315–322). Academic Press.

Wickham, H., Chang, W., Henry, L., Pedersen, T. L., Takahashi, K., Wilke, C., & Woo, K. (2018). *ggplot2: Create Elegant Data Visualisations Using the Grammar of Graphics*. https://cran.r-project.org/package=ggplot2

Xia, L., Lam, S. K., Yan, X., & Chen, D. (2017). How Does Recycling of Livestock Manure in Agroecosystems Affect Crop Productivity, Reactive Nitrogen Losses, and Soil Carbon Balance? *Environmental Science and Technology*, *51*(13), 7450–7457. https://doi.org/10.1021/acs.est.6b06470

Yu, P., He, X., Baer, M., Beirinckx, S., Tian, T., Moya, Y. A. T., Zhang, X., Deichmann, M., Frey, F. P., Bresgen, V., Li, C., Razavi, B. S., Schaaf, G., von Wirén, N., Su, Z., Bucher, M., Tsuda, K., Goormachtig, S., Chen, X., & Hochholdinger, F. (2021). Plant flavones

enrich rhizosphere Oxalobacteraceae to improve maize performance under nitrogen deprivation. *Nature Plants*, *7*(4), 481–499. https://doi.org/10.1038/s41477-021-00897-y

Zhen, Z., Liu, H., Wang, N., Guo, L., & Meng, J. (2014). Effects of Manure Compost Application on Soil Microbial Community Diversity and Soil Microenvironments in a Temperate Cropland in China. *PLoS ONE*, *9*(10), 108555. https://doi.org/10.1371/journal.pone.0108555

Zhu, B., Gutknecht, J. L. M., Herman, D. J., Keck, D. C., Firestone, M. K., & Cheng, W. (2014). Rhizosphere priming effects on soil carbon and nitrogen mineralization. *Soil Biology and Biochemistry*, *76*, 183–192. https://doi.org/10.1016/j.soilbio.2014.04.033

Table 1. Previously determined characteristics of the winter wheat (*Triticum aestivum*) genotypes used in this study

	Byrd	**Cheyenne**	**Snowmass**
Acc. No.[1]	PI 664257	CItr 8885	PI 658597
Origin	Colorado State Univ.	Univ. Nebraska	Colorado State Univ.
Release Date	2011	1933	2009
Stature	Semi-dwarf[2]	Tall	Semi-dwarf
Root architecture[3]	Long, thin	Intermediate	Short, thick
Exudation level[3]	Low	Intermediate	High
Drought Susceptibility[4]	Tolerant	Susceptible	Susceptible

[1] Accession number in the USDA-ARS GRIN database (http://www.ars-grin.gov/).
[2] Semi-dwarf genotypes possess either allele *Rht-B1b* or *Rht-D1b*, and Tall genotypes lack both those alleles.
[3] Based on previous data from Kelly et al. 2022a,b
4From Haley et al.

Table 2. Soil rhizosphere enzyme activities at tillering and heading/flowering stages in wheat genotype x compost amendment field study based in Akron, CO over two growing seasons. Values are average (n = 4) ± standard error in nmol g^{-1} soil hr^{-1}. LAP and PHOS measurements were not taken at tillering in the 2019-2020 season. ANOVA p-values are presented at the bottom of the table.

Year	Sampling Period	Soil Trt.	Variety	TAP[1]	NAG	BG	CB	LAP	PHOS
2020	Tillering	0x	Byrd	76 ± 21	95 ± 18	358 ± 39	105 ± 18		
			Cheyenne	51 ± 9	63 ± 16	283 ± 89	78 ± 27		
			Snowmass	71 ± 8	77 ± 21	314 ± 57	88 ± 21		
		5x	Byrd	96 ± 14	79 ± 14	254 ± 32	83 ± 15		
			Cheyenne	114 ± 24	94 ± 17	277 ± 46	101 ± 23		
			Snowmass	117 ± 16	102 ± 16	330 ± 89	105 ± 10		
	Heading/Flowering	0x	Byrd	70 ± 37	117 ± 60	238 ± 72	64 ± 30	108 ± 51	286 ± 90
			Cheyenne	73 ± 17	62 ± 6	201 ± 18	48 ± 6	77 ± 11	300 ± 55
			Snowmass	63 ± 7	61 ± 8	206 ± 17	48 ± 8	81 ± 14	275 ± 82
		5x	Byrd	97 ± 26	108 ± 43	248 ± 51	68 ± 16	175 ± 64	164 ± 39
			Cheyenne	86 ± 19	88 ± 14	262 ± 36	67 ± 10	143 ± 34	148 ± 24
			Snowmass	93 ± 17	98 ± 31	240 ± 39	62 ± 17	154 ± 44	200 ± 35
2021	Tillering	0x	Byrd	51 ± 10	145 ± 21	372 ± 6	133 ± 15	131 ± 18	428 ± 27
			Cheyenne	54 ± 14	129 ± 25	374 ± 58	125 ± 24	122 ± 20	414 ± 73
			Snowmass	42 ± 10	103 ± 11	324 ± 38	97 ± 13	98 ± 10	380 ± 48
		5x	Byrd	111 ± 35	265 ± 72	519 ± 105	188 ± 54	453 ± 132	305 ± 85
			Cheyenne	101 ± 16	277 ± 87	504 ± 81	166 ± 42	390 ± 67	252 ± 65
			Snowmass	111 ± 25	356 ± 107	557 ± 127	206 ± 61	491 ± 130	313 ± 76
	Heading/Flowering	0x	Byrd	72 ± 25	122 ± 17	295 ± 50	105 ± 16	140 ± 21	304 ± 26
			Cheyenne	52 ± 15	72 ± 8	204 ± 19	68 ± 9	99 ± 10	282 ± 41
			Snowmass	41 ± 9	68 ± 12	177 ± 26	56 ± 11	90 ± 14	274 ± 36
		5x	Byrd	105 ± 18	234 ± 38	411 ± 50	159 ± 32	407 ± 69	197 ± 37
			Cheyenne	94 ± 9	238 ± 36	372 ± 37	138 ± 15	381 ± 32	203 ± 12
			Snowmass	100 ± 8	178 ± 24	338 ± 18	119 ± 10	409 ± 37	203 ± 6
		ANOVA P-values							

Genotype	0.62	0.28	0.68	0.52	0.73	0.85
Soil Treatment	**<0.001**	**<0.001**	**0.0034**	**0.0003**	**0.0001**	**0.0001**
Sampling Period	0.61	0.14	0.39	0.71	**0.0066**	**0.047**
Year	0.3	**<0.001**	**0.0002**	**0.0001**	**0.0001**	**0.0001**
Genotype x Soil Treatment	0.55	**0.099**	0.48	0.63	0.61	0.48

[1] TAP, *L*-Tyrosine aminopeptidase; NAG, N-Acetyl-β-D-glycosaminidase; BG, β-1,4-glucosidase; CB, β-D-cellobiosidase; LAP, *L*-leucine aminopeptidase; PHOS, phosphatase

Table 3. Extractable inorganic N values for rhizosphere soil samples collected from wheat genotypes and different sampling times. Below are ANOVA *p*-values for wheat genotype, long-term soil treatment, and sampling timepoint effects on inorganic N levels in rhizosphere soil samples. Analysis is conducted for 2020 and 20201 separately.

			2020		2021	
Sampling Period	Soil Treatment	Variety	Nitrate (mg kg^{-1})	Ammonium (mg kg^{-1})	Nitrate (mg kg^{-1})	Ammonium (mg kg^{-1})
Tillering	0x	Byrd	21.1 ± 15.0	9.6 ± 1.7	17.1 ± 8.4	1.9 ± 1.1
		Cheyenne	19.4 ± 12.5	12.8 ± 3.9	8.7 ± 2.4	1.5 ± 0.7
		Snowmass	9.8 ± 4.7	7.8 ± 2.9	9.3 ± 3.9	1.9 ± 0.9
	5x	Byrd	25.3 ± 6.8	1.2 ± 0.2	25.0 ± 6.3	3.1 ± 1.2
		Cheyenne	57.2 ± 26.8	3.2 ± 1.2	19.5 ± 4.2	1.4 ± 0.1
		Snowmass	22.5 ± 10.5	5.1 ± 0.8	23.6 ± 4.0	2.1 ± 0.4
Heading/flowering	0x	Byrd	15.1 ± 9.1	5.6 ± 1.1	3.5 ± 0.4	1.5 ± 0.0
		Cheyenne	13.4 ± 7.6	7.3 ± 2.0	3.8 ± 1.0	1.3 ± 0.1
		Snowmass	9.6 ± 4.8	4.7 ± 1.5	2.7 ± 0.3	1.3 ± 0.0
	5x	Byrd	35.6 ± 7.7	1.6 ± 0.5	20.1 ± 4.9	2.2 ± 0.6
		Cheyenne	36.2 ± 15.7	2.3 ± 0.6	14.6 ± 3.6	2.1 ± 0.3
		Snowmass	32.5 ± 2.8	3.1 ± 0.4	19.0 ± 1.9	1.9 ± 0.2
	ANOVA *P*					
		Genotype	0.75	0.53	0.43	0.59
		Soil	**0.01**	**0.001**	**<0.001**	**0.02**
		Timepoint	0.46	**<0.001**	**<0.001**	0.75
		Genotype x Soil	0.97	0.30	0.44	0.87

Supplemental Material

Soil management legacy interacts with wheat genotype to determine access to organic N in a dryland system

Courtland Kelly[1,2], Patrick F. Byrne[1], Meagan Schipanski[1], Joel Schneekloth[3], Francisco Calderón[4], Steven. J. Fonte[1]

[1] Department of Soil and Crop Sciences, Colorado State University, Fort Collins, CO

[2] Physical and Life Sciences Directorate, Lawrence Livermore National Laboratory, Livermore, CA

[3] US Central Plains Research Station, Colorado State University, Akron, CO

[4] Columbia Basin Agricultural Research Center, Oregon State University, Adams, OR, USA

Table S1. Soil characteristics (0 – 30 cm) for different long-term compost-amended soil treatments, applied every two years for 10 years at a rate of 0 t ha^{-1} (0x) or 109 t ha^{-1} (5x). The final compost application occurred in fall 2019.

Soil Management	SOC ($g\ kg^{-1}$)	Total N ($g\ kg^{-1}$)	$\delta^{15}N$	NO_3-N ($mg\ kg^{-1}$)	NH_4-N ($mg\ kg^{-1}$)	Extractable P ($mg\ kg^{-1}$)[a]	1:1 pH
No compost	14.1	1.9	14.66	21.8	4.5	5.1	7.3
5x Compost	19.0	2.4	26.63	30.7	6.8	47.3	7.2

Table S2. Monthly weather data during two field growing seasons of winter wheat in Akron, CO.

		Month												
Season		**Aug**	**Sep**	**Oct**	**Nov**	**Dec**	**Jan**	**Feb**	**Mar**	**Apr**	**May**	**Jun**	**Jul**	**Total**
2019-2020	Avg. Max Temp (C)	30.5	28.9	14.8	9.7	6.3	7.9	5.8	11.6	15.4	21.6	31.4	32.2	
	Avg. Min Temp (C)	14.7	11.6	-1.7	-4.8	-5.9	-7.6	-9.0	-2.3	-1.5	6.2	12.4	15.4	
	Total Precip (mm)	60.5	6.9	13.0	27.9	2.0	4.1	6.6	16.5	9.9	76.5	31.8	17.5	273.1
2020-2021	Avg. Max Temp (C)	33.0	25.6	16.7	14.0	5.8	5.1	0.9	10.5	14.2	19.2	28.4	32.0	
	Avg. Min Temp (C)	14.9	8.6	-0.5	-2.4	-7.4	-7.2	-11.4	-3.1	-0.4	7.0	12.8	14.4	
	Total Precip (mm)	33.0	32.0	7.6	7.1	11.2	7.9	10.9	57.7	87.1	176.3	18.3	11.7	460.8
113 Year Mean	Avg. max Temp (C)	30.6	25.8	18.8	10.6	4.8	3.8	6.0	10.3	15.9	21.2	27.6	31.7	
	Avg. Min Temp (C)	13.6	8.4	1.7	-4.8	-9.3	-10.4	-8.3	-4.6	0.3	5.9	11.2	14.6	
	Total Precip (mm)	53.9	31.7	23.0	13.6	10.4	8.3	9.3	21.6	42.0	76.3	61.9	65.5	417.5

Table S3. Wheat yield from the excluded 2019-2020 season. Despite supplemental irrigation in Fall 2019 to improve germination, wheat yields were far below average. Values are mean ± standard error.

Soil Treatment	Genotype	Wheat grain yield (kg ha^{-1})	Wheat straw yield (kg ha^{-1})	Total wheat biomass (kg ha^{-1})
0x	Byrd	881 ± 158	5,507 ± 899	6,388 ± 1,049
	Cheyenne	612 ± 184	5,230 ± 323	5,842 ± 470
	Snowmass	754 ± 153	4,732 ± 551	5,487 ± 679
5x	Byrd	521 ± 261	5,453 ± 1,701	5,974 ± 1,949
	Cheyenne	691 ± 223	6,691 ± 809	7,381 ± 977
	Snowmass	714 ± 253	5,115 ± 1,200	5,829 ± 1,347
P values				
Genotype		0.88	0.49	0.62
Soil Treatment		0.44	0.40	0.55
Genotype x Soil Treatment		0.42	0.66	0.61

Table S4. Nitrogen content and total uptake of wheat grain and straw in wheat genotype x compost treatment field study in Akron, CO. Samples were collected from 1 m^2 microplots amended with ^{15}N labelled cover crop residues. Values represent the means (n = 4) ± standard error for wheat sampled in the 2021 season.

Soil Treatment	Genotype	Grain N conc. (g kg^{-1})	Straw N conc. (g kg^{-1})	Grain N uptake (g m^{-2})	Straw N uptake (g m^{-2})	Total N uptake (g m^{-2})
0x	Byrd	30.0 ± 2.0	9.4 ± 1.5	6.0 ± 1.9	9.6 ± 2.0	15.6 ± 2.2
	Cheyenne	27.3 ± 0.7	9.5 ± 1.8	7.6 ± 2.0	10.6 ± 1.6	18.2 ± 1.7
	Snowmass	29.5 ± 3.0	9.5 ± 1.6	9.0 ± 1.4	10.6 ± 0.9	19.6 ± 0.8
5x	Byrd	30.3 ± 1.5	16.4 ± 0.3	5.8 ± 1.3	19.7 ± 0.7	25.5 ± 1.8
	Cheyenne	29.7 ± 1.0	17.3 ± 1.3	4.9 ± 0.8	20.2 ± 3.7	25.1 ± 4.4
	Snowmass	29.1 ± 2.1	19.6 ± 1.3	3.9 ± 0.8	24.6 ± 3.3	28.5 ± 3.3
P values						
Genotype		0.67	0.5	0.92	0.43	0.29
Soil Treatment		0.64	**<0.001**	**0.03**	**<0.001**	0.12
Genotype x Soil Treatment		0.75	0.53	0.26	0.59	0.56

Table S5. Rhizosphere microbiome diversity metrics for bacterial/archaeal markers and fungal marker genes. Values are means ± standard error, and ANOVA analysis results (*p*-values) are presented at the bottom of the table. Shannon and Pielou diversity indices are presented, and Richness is expressed as total features per sample.

				Bacteria/Archaea (16S)			Fungi (ITS)		
Year	Timepoint	Soil.trt	Variety	Shannon	Pielou	Richness	Shannon	Pielou	Richness
2020	Tillering	0x	Byrd	9.0 ± 0.10	0.91 ± 0.01	1,003 ± 68	4.9 ± 0.49	0.60 ± 0.05	283 ± 28
			Cheyenne	8.9 ± 0.13	0.90 ± 0.01	952 ± 40	5.5 ± 0.26	0.67 ± 0.03	313 ± 13
			Snowmass	8.8 ± 0.05	0.89 ± 0.00	1,006 ± 47	5.4 ± 0.19	0.66 ± 0.02	281 ± 22
		5x	Byrd	8.8 ± 0.11	0.88 ± 0.01	979 ± 51	4.9 ± 0.35	0.61 ± 0.04	242 ± 29
			Cheyenne	8.7 ± 0.12	0.87 ± 0.01	997 ± 56	5.4 ± 0.07	0.67 ± 0.01	255 ± 9
			Snowmass	8.3 ± 0.19	0.85 ± 0.02	840 ± 40	5.2 ± 0.13	0.66 ± 0.02	227 ± 6
	Heading/Flowering	0x	Byrd	9.0 ± 0.12	0.90 ± 0.01	1,032 ± 46	5.1 ± 0.46	0.61 ± 0.05	304 ± 32
			Cheyenne	9.0 ± 0.04	0.91 ± 0.00	1,006 ± 3	5.6 ± 0.37	0.67 ± 0.04	321 ± 18
			Snowmass	9.2 ± 0.09	0.91 ± 0.00	1,126 ± 63	5.5 ± 0.32	0.66 ± 0.03	330 ± 16
		5x	Byrd	8.8 ± 0.33	0.89 ± 0.02	956 ± 130	4.6 ± 0.18	0.60 ± 0.01	222 ± 31
			Cheyenne	9.2 ± 0.04	0.90 ± 0.00	1,156 ± 18	5.4 ± 0.13	0.67 ± 0.01	271 ± 11
			Snowmass	9.0 ± 0.15	0.90 ± 0.00	1,006 ± 88	4.9 ± 0.17	0.62 ± 0.01	234 ± 27
2021	Tillering	0x	Byrd	9.4 ± 0.17	0.91 ± 0.01	1,294 ± 227	4.2 ± 0.27	0.53 ± 0.03	264 ± 21
			Cheyenne	9.2 ± 0.02	0.91 ± 0.00	1,131 ± 22	4.7 ± 0.36	0.58 ± 0.04	301 ± 21
			Snowmass	9.3 ± 0.05	0.91 ± 0.00	1,162 ± 39	5.1 ± 0.20	0.62 ± 0.02	303 ± 15
		5x	Byrd	9.1 ± 0.16	0.90 ± 0.01	1,192 ± 88	4.9 ± 0.12	0.65 ± 0.02	191 ± 6
			Cheyenne	9.1 ± 0.09	0.90 ± 0.01	1,080 ± 34	4.4 ± 0.12	0.60 ± 0.02	168 ± 8
			Snowmass	9.1 ± 0.15	0.91 ± 0.00	1,038 ± 110	4.5 ± 0.15	0.61 ± 0.02	163 ± 11
	Heading/flowering	0x	Byrd	9.5 ± 0.10	0.92 ± 0.00	1,354 ± 132	4.6 ± 0.44	0.56 ± 0.05	292 ± 20
			Cheyenne	9.2 ± 0.12	0.91 ± 0.01	1,099 ± 58	5.2 ± 0.31	0.62 ± 0.03	356 ± 28
			Snowmass	9.4 ± 0.05	0.91 ± 0.00	1,226 ± 42	5.3 ± 0.23	0.64 ± 0.03	322 ± 14
		5x	Byrd	9.1 ± 0.15	0.90 ± 0.01	1,162 ± 110	4.6 ± 0.24	0.62 ± 0.02	189 ± 19
			Cheyenne	9.1 ± 0.11	0.90 ± 0.01	1,102 ± 96	4.3 ± 0.14	0.57 ± 0.02	177 ± 7
			Snowmass	9.0 ± 0.08	0.89 ± 0.00	1,111 ± 44	3.7 ± 0.41	0.50 ± 0.05	170 ± 7

	ANOVA P						
	Genotype	0.46	0.6	0.42	**0.099**	0.14	0.18
	Soil	**<0.001**	**< 0.001**	0.12	**0.007**	0.92	**< 0.001**
	Timepoint	**0.001**	**< 0.001**	**0.036**	0.86	0.43	**0.02**
	Year	**<0.001**	**< 0.001**	**< 0.001**	**< 0.001**	**< 0.001**	**0.002**

Table S5. Gravimetric water content of soil from rhizosphere (Tillering & Heading) and surface 0-30 cm (Harvest) samples. All values are expressed as percent of dry soil in mean ± standard error. ANOVA results (*p*-values) are presented at the bottom of the table.

			Timepoint		
Year	**Soil Treatment**	**Variety**	**Tillering**	**Heading/Flowering**	**Harvest**
2020	0x	Byrd	24.0 ± 1.5	7.8 ± 0.9	7.2 ± 0.9
		Cheyenne	25.5 ± 2.7	7.4 ± 0.8	8.0 ± 0.4
		Snowmass	25.0 ± 1.3	8.1 ± 0.9	6.4 ± 1.1
	5x	Byrd	25.6 ± 1.6	9.3 ± 1.4	7.3 ± 1.2
		Cheyenne	27.3 ± 1.7	7.9 ± 1.0	7.5 ± 1.6
		Snowmass	29.4 ± 1.9	8.6 ± 1.0	7.5 ± 1.5
2021	0x	Byrd	25.6 ± 1.8	17.9 ± 2.3	8.0 ± 0.6
		Cheyenne	28.5 ± 1.9	19.0 ± 3.0	9.1 ± 0.3
		Snowmass	25.5 ± 1.3	16.0 ± 2.5	8.3 ± 0.2
	5x	Byrd	32.0 ± 1.6	23.0 ± 3.5	8.2 ± 0.3
		Cheyenne	32.5 ± 2.1	23.4 ± 4.7	9.1 ± 0.3
		Snowmass	30.8 ± 1.7	20.5 ± 2.5	9.2 ± 0.5
ANOVA P					
Genotype	0.54				
Soil	**< 0.001**				
Year	**< 0.001**				
Sample Period	**< 0.001**				
Soil x Year	0.11				

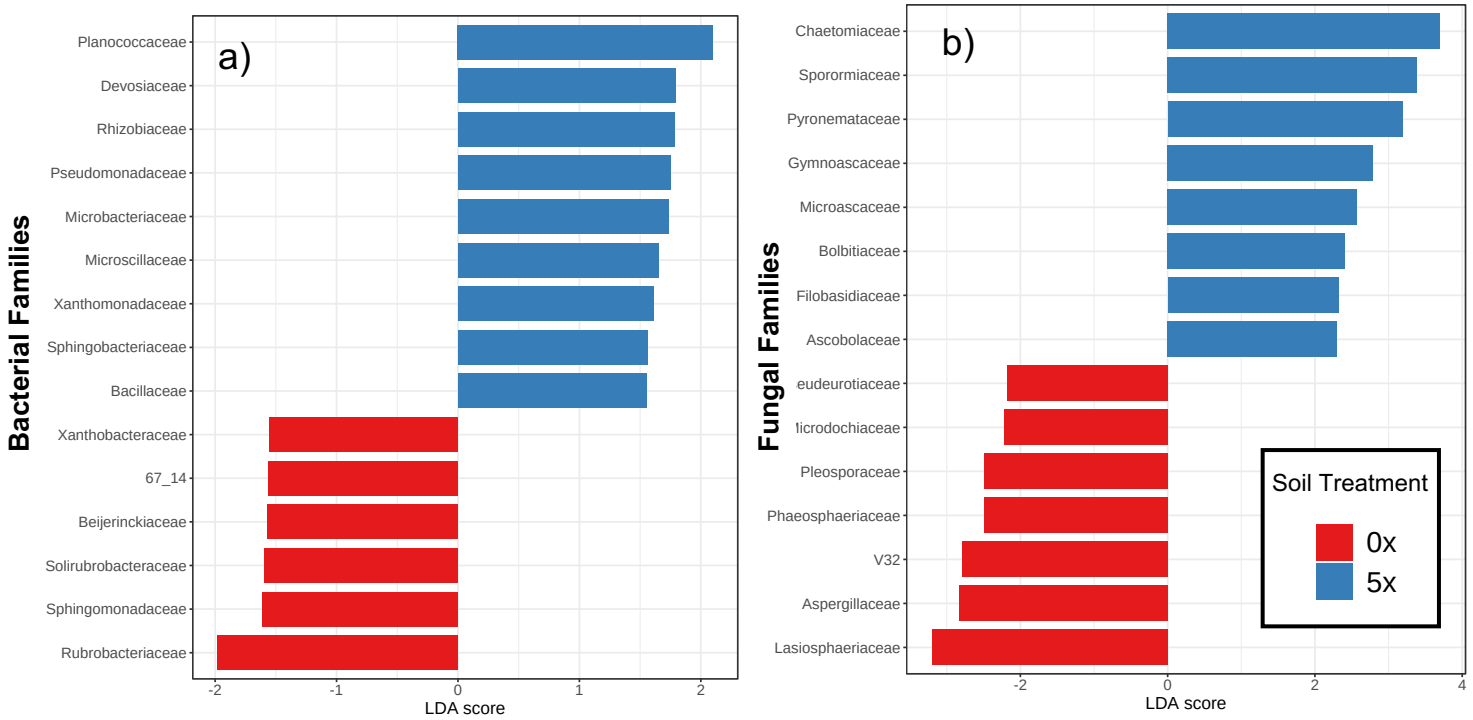

Figure S1. Linear Discriminate Analysis Effect Size (LEfSe) analysis results for family-level a) bacterial communities based on 16S amplicon sequencing and b) fungal families based on ITS sequencing. Analysis identifies families important for indicating grouping by soil compost treatment (bar colors), with larger absolute LDA scores indicating greater importance. Data shown for both years.

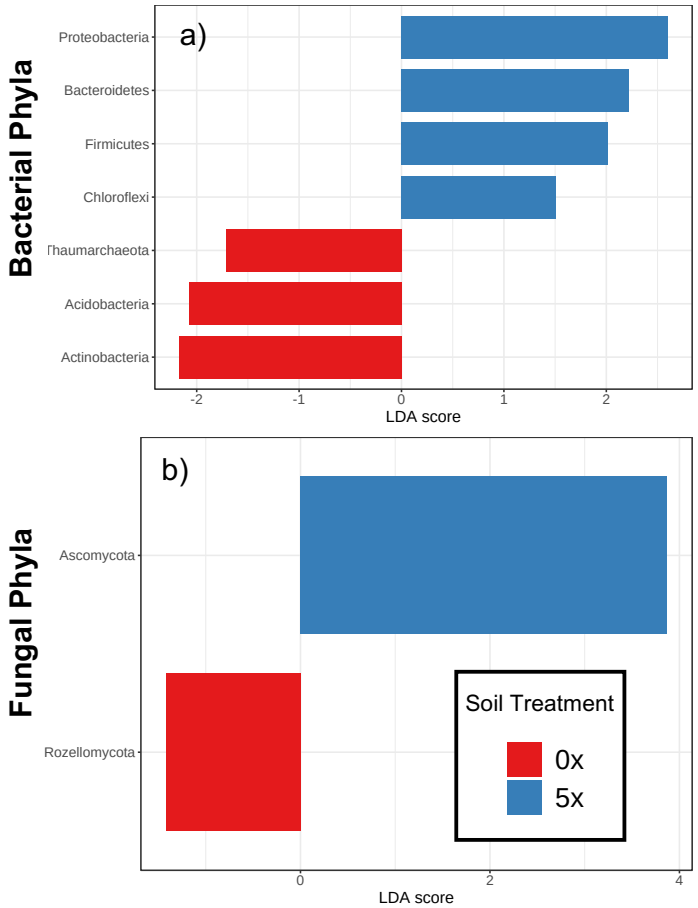

Figure S2. Linear Discriminate Analysis Effect Size (LEfSe) analysis results for a) bacterial phyla based on 16S amplicon sequencing and b) fungal phyla based on ITS sequencing. Analysis indicates families important for indicating groups (bar colors), with higher absolute LDA scores indicating greater importance.

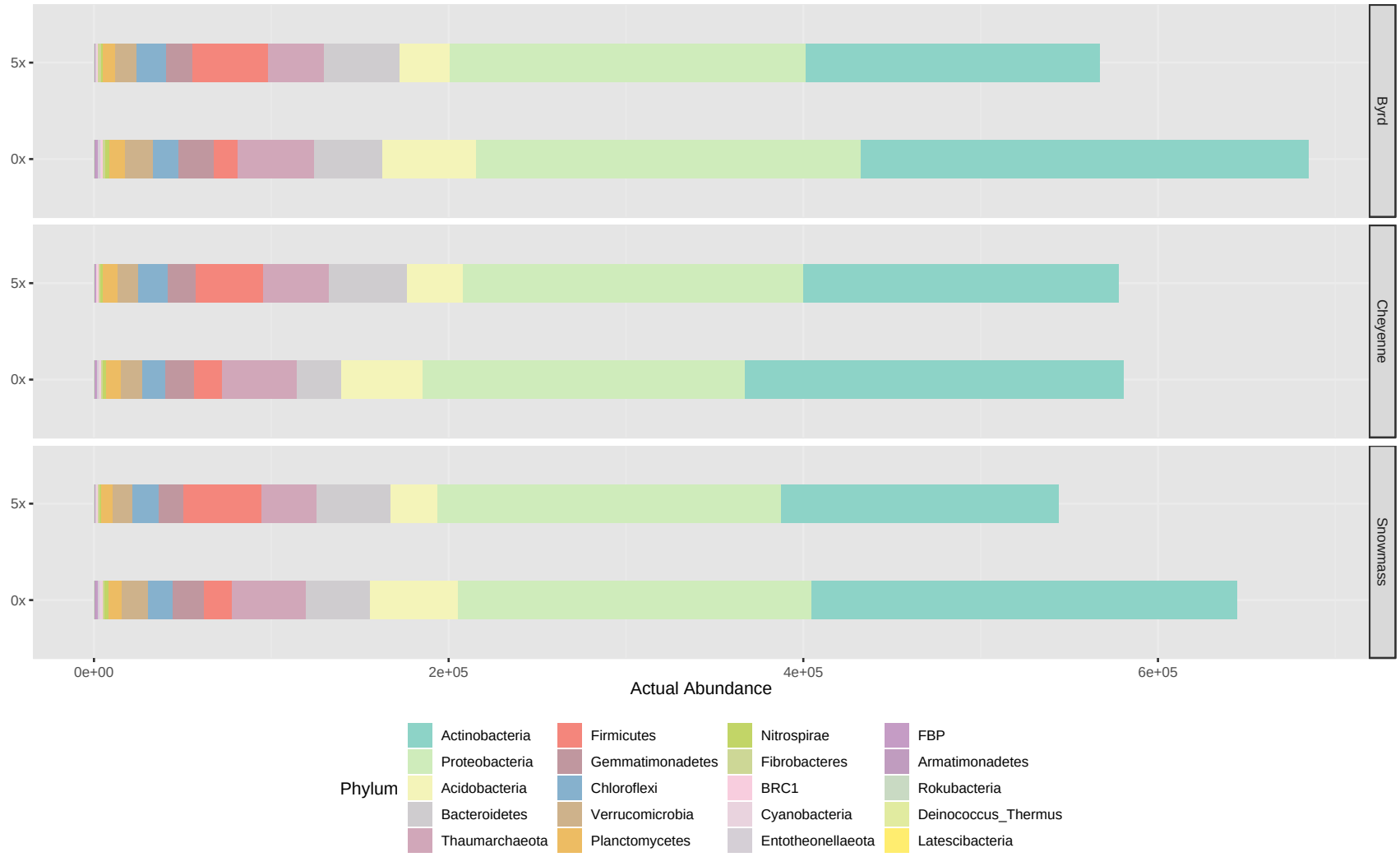

Figure S3. Bacterial phylum relative abundances based on 16S sequencing. Bar lengths depict merged (summed) abundances for each soil-by-genotype combination and are colored by phylum.

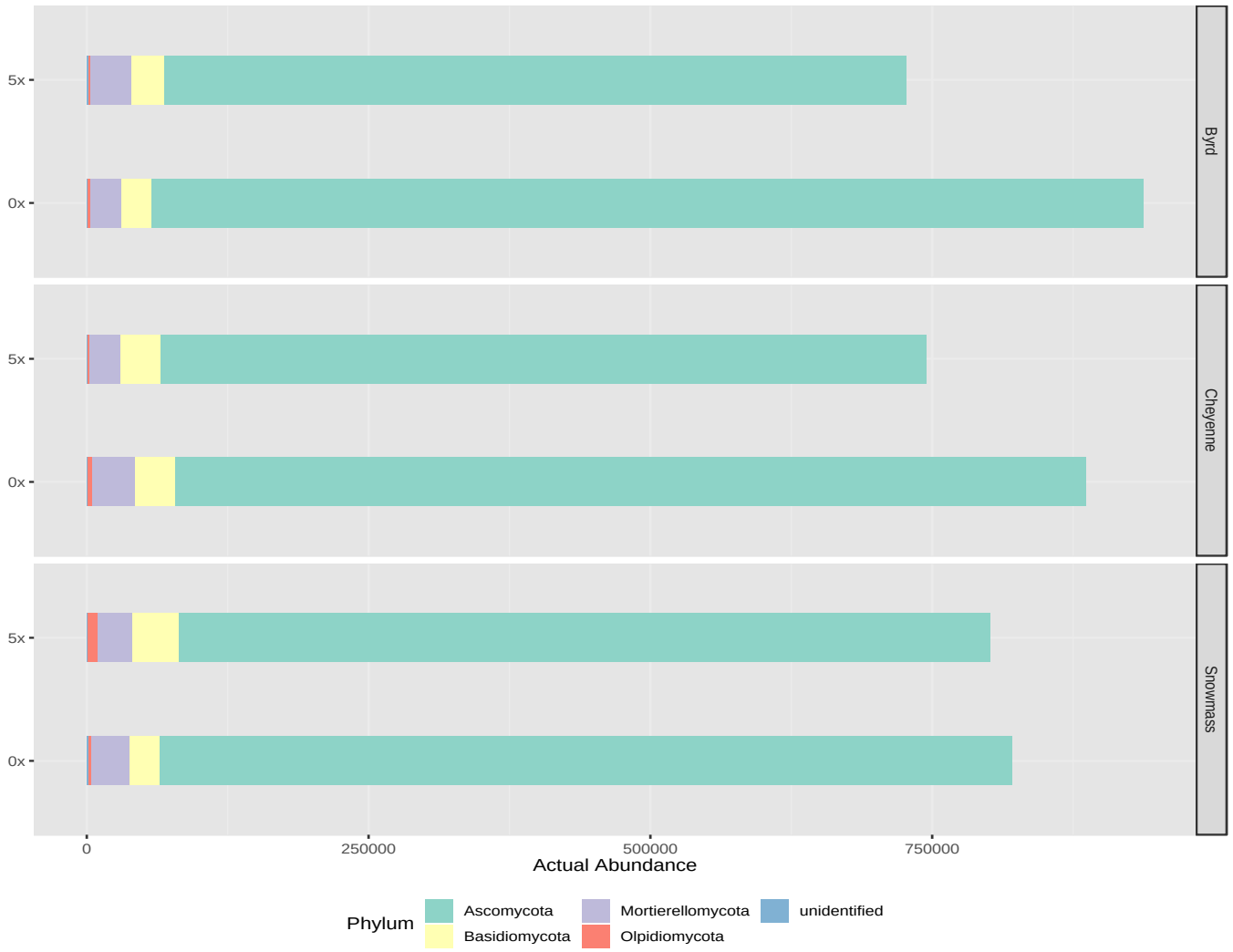

Figure S4. Fungal abundances based on ITS sequencing. Bar lengths depict the sum total relative abundance across all samples in each soil-by-genotype group.